

# INFLUENCE OF AN INCLUSION ON MULTI-PASS COPPER SHAPED-WIRE DRAWING BY 2D FINITE ELEMENT ANALYSIS

*S. Norasethasopon*

*Department of Mechanical Engineering, Faculty of Engineering, King Mongkut's Institute of Technology  
Bangkok, Thailand*

*K. Yoshida*

*Department of Precision Mechanics, School of Engineering, Tokai University  
Kanagawa, Japan*

**(Received: December 20, 2002 – Accepted in Revised Form: June 25, 2003)**

**Abstract** The size and length effects of an inclusion on multi-pass copper shaped-wire drawing were investigated. For this purpose, an experimental investigation on optimal die half-angle was conducted. Based on experimental data of optimal die half-angle, wire and inclusion deformations, drawing and hydrostatic stress of copper shaped-wires that contain an inclusion were calculated by two-dimensional finite element analysis. As a result, during drawing of a wire containing an inclusion, necking occurred. The effects of inclusion size and length on drawing stress and maximum hydrostatic tensile stress in front of inclusion during multi-pass copper shaped-wire drawing were carried out. The maximum hydrostatic tensile stress occurred on wire centerline in front of inclusion for single-pass drawing. When the wire was repeatedly drawn, the maximum hydrostatic tensile stress regions symmetrically separated out and were at both side of wire centerline in front of inclusion. Symmetrical double crack easily occurred in those regions.

**Key Words** Multi-Pass Drawing, Internal Fracture, FEA, Copper Shaped-Wire, Inclusion, Drawing Stress, Hydrostatic Stress

**چکیده** اثرات اندازه و طول یک آخال بر کشش مفتولی چند پاس سیم پروفیل مسی بررسی شد. بدین منظور، نیم زاویه بهینه حدیده از طریق تجربی بررسی گردید. به کمک نتایج تجربی مربوط به حدیده نیم زاویه بهینه، تغییر شکلهای سیم و آخال و تنشهای کششی و هیدرواستاتیک سیم مسی شکل داده شده ای که دارای یک آخال است، با استفاده از آنالیز اجزای محدود دو بعدی محاسبه گردید. در نتیجه ملاحظه شد که در خلال کشش سیم دارای آخال، گلوئی شدن رخ می دهد. اثرات اندازه طول آخال بر تنش کششی و ماکزیمم تنش کششی هیدرواستاتیک در جلوی آخال در خلال کشش متوالی چند پاس سیم پروفیل مسی مورد بررسی قرار گرفت. ملاحظه شد که ماکزیمم تنش کششی هیدرواستاتیک روی خط میانی سیم و در جلوی آخال برای کشش تک پاس اتفاق می افتد. زمانی که کشش سیم به دفعات تکرار می شود، مناطق ماکزیمم تنش کششی هیدرواستاتیک بطور قرینه از یکدیگر فاصله یافته و در دو طرف خط میانی سیم در جلوی آخال قرار می گیرند. در این مناطق به راحتی ترکهای مضاعف قرینه شکل می گیرند.

## 1. INTRODUCTION

A method of superfine wire manufacturing is to use a wire rod as the raw material and repeatedly subjecting the wire rod to wire drawing and heat treatment. Another method that is frequently used

in superfine wires manufacturing is to obtain a metallic fibre directly from molten metal. Except for certain materials, the forming method as it provides favourable wire quality, stability and processing cost manufacture most practically used metallic products. The various

TABLE 1. Minimum Diameter and Use of Superfine Wires in Market and Laboratory in Japan [1].

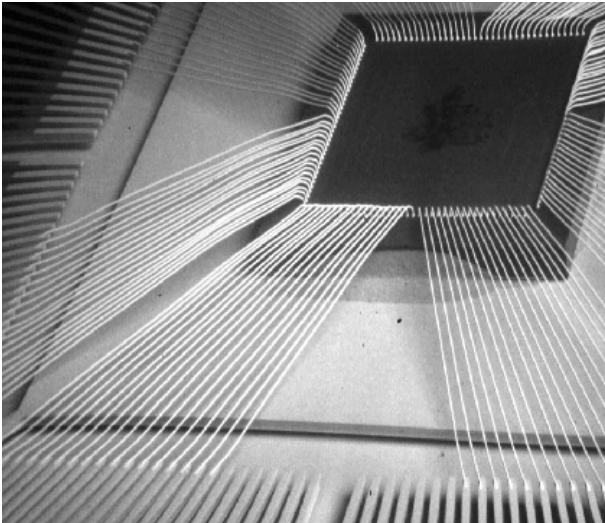
Materials	Diameter [ $\mu\text{m}$ ]		Use of Products
	Market	Laboratory	
Special Mild	~15	~12	Fishing line
Low-Carbon	~100	----	Screw, pin, bolt
High-Carbon	150 ~ 16	100 ~ 10	Steel cord, sawing wire cable, spring
Stainless Steel	30 ~ 15	20 ~ 10	Screen mesh, mesh of filter wire rope
Titanium	100 ~ 50	10 ~ 5	Mesh of filter, wire rope stiffening wire
Shape-Memory	~ 40	~ 10	Fishing line, antenna
Amorphous	20 ~ 15	30 ~ 10	Sensor, stiffening wire
Gold	50 ~ 15	~ 15	Bonding wire
Copper	15 ~ 10	15 ~ 7	Electronic wire, bonding wire
Aluminum	30 ~ 20	~ 20	Electronic wire, bonding wire

superfine wires used in commercially available products and research work in Japan [1] are shown in Table 1. Superfine steel wires are used for printing meshes, filters, steel cords, saw wires, wire ropes, precision springs, and precision screws and pins. Superfine non-ferrous wires are used for semiconductor bonding wires as shown in Figure 1(a), magnet wires as shown in Figure 1(b), materials for electronic components and electrode wires for electrical-discharge processing. Superconducting wires have been used in various fields such as in the medical field for magnetic resonance imaging (MRI), the field of transportation for linear motor cars and the electric power field for nuclear fusion

Superfine wire processing requires a large numbers of drawing pass and intermediate softening heat treatments. Sometimes the internal defects of wires such as inclusions, voids, cracks and central-bursts or chevron formations occur, resulting in both wire breakage and high manufacturing costs. They are usually not visible from the surface because they are inside. Non-destructive testing such as x-ray radiography or ultrasonic testing may be required to detect these defects. Central bursts or chevrons are internal

defects that appear on the longitudinal cross section of the wire as arrowhead or chevron-shaped voids that point in the direction of metal flow. They are usually resulted from small reduction of non-strain-hardening metals such as severely cold-worked metal, since cold working reduces the strain-hardening exponent. In multi-pass operations, chevroning usually occurs when a light reduction follows a heavy one. They occur with relatively small reductions, large die angles, high surface friction, and subsequent to previous severe cold working. This defect can be prevented by increasing the reduction, decreasing the die half-angle, decreasing the friction, and increasing the strain hardening capacity of the material by annealing or material selection [2]. Avitzur [3] has presented an explanation of the cause of central-burst or chevron formation in wire drawing and the limitations placed on these processes.

A reason for the high manufacturing costs of superfine wires is the breakage of wires during processing. The causes of wire breakage have been widely studied for a long time. But, there are a few published reports. Many researchers have investigated optimal wire drawing conditions with respect to various factors such as die angle,



a) Bonding wires



b) Magnet wire for wristwatch (Courtesy of SEIKO Corp.)

**Figure 1.** Use of superfine wires in the fields of precision equipment and semiconductors [10].

reduction, annealing conditions and selection of lubricant for the defects in production process. Avitzur [3-5] proposed the conditions under which internal fracture occurred using an energy method. Roger [6] and Yoshida [7] studied the occurrence of damage and voids during the drawing using a slip-line field method. Chen [8] and Yoshida [1,7,9,10] studied the causes of internal cracking and how such cracks grow, using finite element analysis (FEA) and proposed some processing

conditions to prevent defects. Structural damage during wire drawing for a given microstructure generally correlates well with the amount of hydrostatic stress that develops within the material. A high hydrostatic tensile component will tend to nucleate voids or cracks in a body and will enhance their growth and also probable structural damage. Raskin [11] reported the causes of wire breakage during copper wire drawing based on his survey of 673 wire breaks, that 52%, 13%, 13%, 5%, 5%, and 12% are attributable to inclusion, central bursting or cupping, tension break, weld break, silver break and others, respectively, as shown in Figure 2. The most important problem of wire breakage during copper wire drawing is wire breakage due to inclusions as shown in Figure 3.

A lot of research efforts have been made for development of ultra small motors in Japan. To further improve the performance at the efficiency of such motors, a cross-section of the magnet wire for the motor needs to be changed from circular to square. At present, the size of the square is suggested to be in a range of 300 to 500 micrometer [12].

## 2. BASIC THEORY OF WIRE DRAWING

The wire drawing processes are classified as indirect compression processes, in which the major forming stress results from the compressive stress as a result of the direct tensile exerted in drawing. The converging die surface in the form of a truncated cone is used. The analytical or mathematical solutions [2] are obtained by free body equilibrium method. By summing the forces in the wire drawing direction of a free body equilibrium diagram at an element in the reduction zone, the longitudinal stress is obtained. Summing the forces in the radial direction, the radial or die-breaking stress is obtained. Then combining those results, integrating the resulting differential equation, and simplifying, the equation for the average drawing stress is obtained.

The finite element method is a powerful tool for the numerical solution of wire drawing. With the advance in computer technology, wire drawing

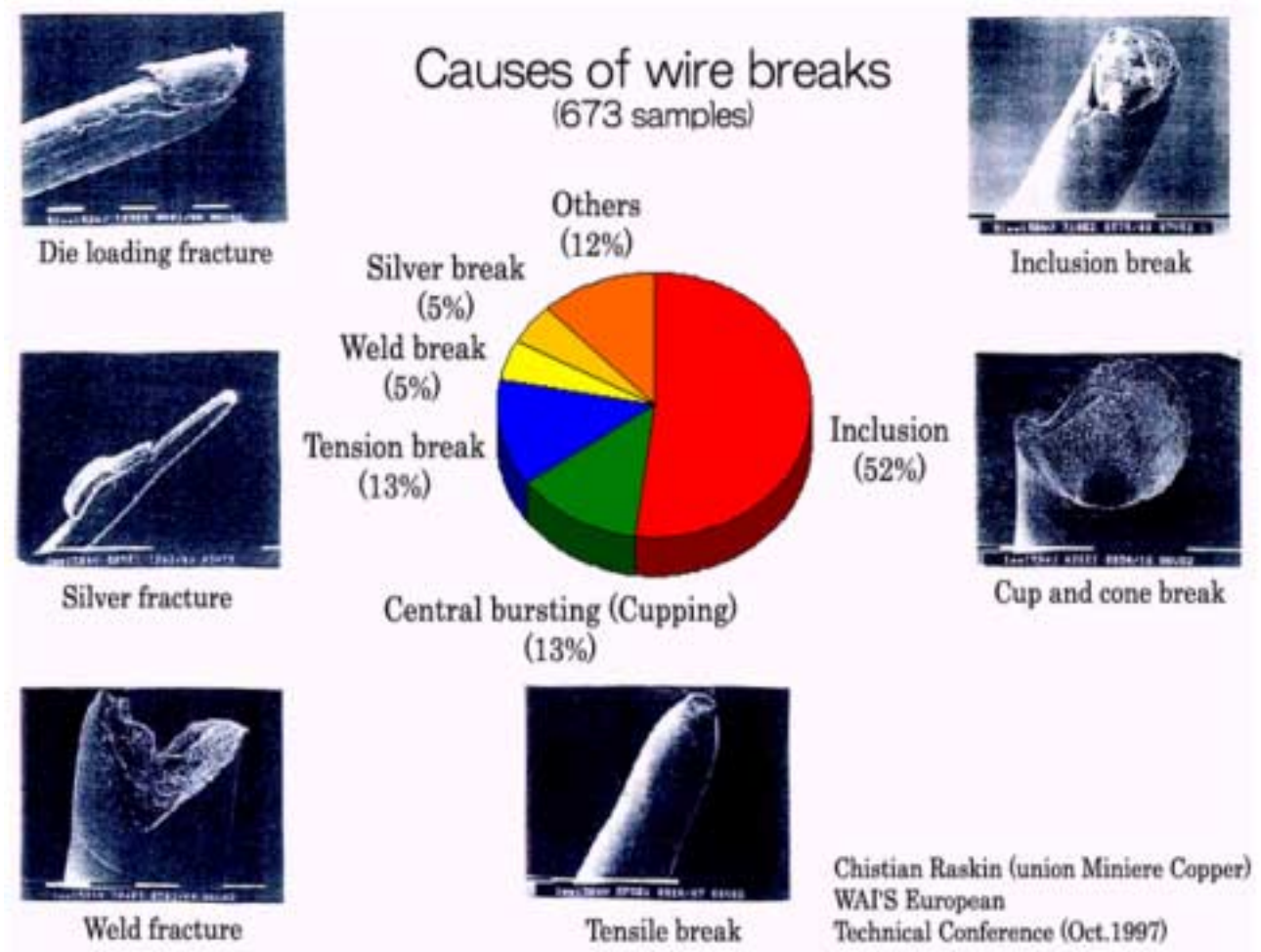


**Figure 2.** Causes of wire breakage during copper wire drawing [11].

can be modeled with relative ease. In this FEA have the following six steps. First step, Shape Functions, the finite element method expresses the unknown field in terms of the nodal point unknowns by using the shape functions over the domain of the element. Second step, Material Loop, the finite element method expresses the dependent flux fields such as the strain or stress in terms of the nodal point unknowns. Third step, Element Matrices, the finite element method equilibrates each element with its environment. Fourth step, assembly, the finite element method assembles all elements to form a complete structure in such a manner to equilibrate the structure with its environment. Fifth step, Solve

Equations, the finite element method specifies the boundary conditions, namely, the nodal point values on the boundary and the system equations are partitioned. Sixth step, Recover, the finite element method recovers the stresses by substituting the unknown nodal values found in fifth step back into second step to find the dependent flux fields such as strain, stress, etc.

### 3. OPTIMAL DIE HALF-ANGLE EXPERIMENT

The author [13] investigated the effects of die half-angle on drawing stress while wire drawing by



**Figure 3.** Wire breakage due to an inclusion: a)  $D_0 = 54 \mu\text{m}$  b)  $D_0 = 60 \mu\text{m}$  [1].

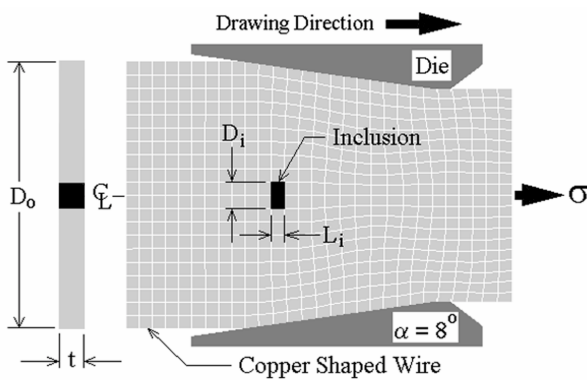


**Figure 4.** FEA model was used in this investigation.

experiment to find out the optimal dies half-angle of copper wire. The properties of copper wire with a diameter of 5.5 mm used as specimens are as follow:  $E = 120000 \text{ MPa}$ ,  $\sigma_Y = 150 \text{ MPa}$ , and  $\nu = 0.3$ . The reduction/pass of copper wire drawing was 17.4 % so drawn wire had a diameter of 5 mm.

In this experiment, the various die half-angles: 4, 6, 8, 10, and 12 degrees were used. The relation between drawing stress on copper wire and the die half-angle was obtained. For a die half-angle of 4 degrees, the drawing stress was so large that the copper wire was finally broken. For the die half-angle of 6, 8, 10, and 12 degrees, the drawing stress decreased while the die half-angle increased. The drawing stress reached a minimum at the die half-angle of 8 degrees then increased while the

**TABLE 2. Material Properties and Drawing Conditions Used for FEA.**

	Copper (wire)	WC (inclusion)
Young's modulus E (MPa)	120000	1000000
Yield stress Y (MPa)	150	1000
Poisson's ratio $\nu$	0.3	0.22
Die half-angle $\alpha$ (deg)	8	
Reduction perpass R/P (%)	20	
Coefficient of friction $\mu$	0.05	

die half-angle increased. It was found that the minimum drawing stress occurred at a die half-angle of 8 degrees. So the optimal die half-angle for copper wires drawing was at 8 degrees [13].

#### 4. FEA RESULTS AND DISCUSSION

A two-dimensional finite element method was used to analyze the effect of an inclusion on copper shaped-wire drawing. The analytical model used in this analysis was shown in Figure 4. The black part is the inclusion of copper shaped-wire. The inclusion is located on the copper shaped-wire centerline. The model solution was obtained by using MSC.MARC finite element program. The numerous built-in features of the MSC.MARC finite element program provide flexibility in the model setup. The element type, wire and inclusion material, die material, friction model and analysis type were set as quadrilateral, isotropic (elastic-plastic), rigid, Coulomb and plane strain (large deformation), respectively.

The details of the author's assumption in this analysis were shown in Table 2. The inclusion length  $L_i/D_0$ , the ratio of the inclusion length to the dimension of wire cross-section: 0.05, 0.1, 0.2, 0.3

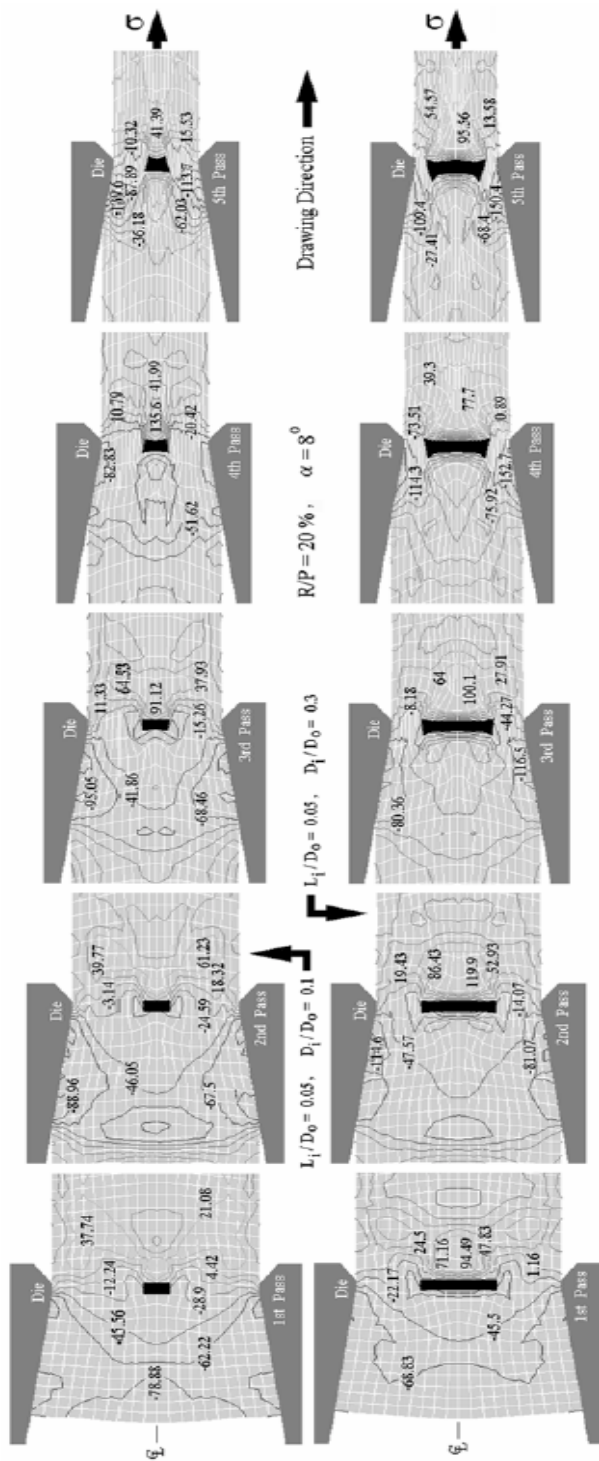


**Figure 5.** Hydrostatic stress distribution of copper shaped-wire containing an inclusion during multi-pass drawing.

and 0.4 were used. The inclusion size  $D_i/D_0$ , the

ratio of dimension of inclusion cross-section to the dimension of wire cross-section: 0.1, 0.2, 0.3, and 0.4 were also used. The die half-angle ( $\alpha$ ), reduction per pass (R/P) and coefficient of friction ( $\mu$ ) were set at 8 degrees, 20 %, and 0.05, respectively. The authors assumed that the inclusion and the copper matrix were joined at the boundary, and the used materials were not work-hardened during the process. This analysis, the wire was considered as a copper shaped-wire with hard inclusion subjected to steady deformation.

**Inclusion Size Effects** For inclusion size ( $D_i/D_0$ ) equal to 0.1 and 0.3, the distributions of hydrostatic stress and deformation behavior of copper shaped-wires with an inclusion for inclusion length ( $L_i/D_0$ ) equal to 0.05 during the whole five times of drawing pass were obtained as shown in Figure 5. The maximum hydrostatic tensile stress ( $\sigma_t/Y$ ) and drawing stress ( $\sigma/Y$ ) of copper shaped-wires containing an inclusions for  $D_i/D_0 = 0.1, 0.2, 0.3,$  and  $0.4$  where  $L_i/D_0 = 0.05$  were also obtained in Figure 6 (a) and Figure 7 (a), respectively.

For first pass drawing, the inclusion was negligibly deformed because of its hardness, resulting in large copper deformation. The inclusion deformation occurred when copper shaped-wire was repeatedly drawn and it was deformed to be “crown” shape. For large and short inclusion as shown in Figure 5, the inclusion was deformed to be “crown” shape and also bent. The bending of inclusion was not occurred for small inclusion. The deformed small inclusion shape, “crown” shape, was inversion when compare with deformed large inclusion shape. As the inclusion passes through the die, necking due to an inclusion wire drawing occurred at some parts of the wire. The necking occurred on the copper shaped-wire surface in front of inclusion near inclusion boundary and its magnitude increase as  $D_i/D_0$  increase. While drawing the wires containing an inclusion, it was found that the  $\sigma_t/Y$  in front of the inclusion increase as  $D_i/D_0$  increase.

The  $\sigma_t/Y$  increases as  $D_i/D_0$  increase in first and second pass drawing was shown in Figure 6 (a). The  $S_i/D_0$  slightly influenced on  $\sigma_t/Y$ . In third pass drawing, the  $\sigma_t/Y$  in case of  $D_i/D_0 = 0.4$  was lower than the  $\sigma_t/Y$  in case of smaller inclusion

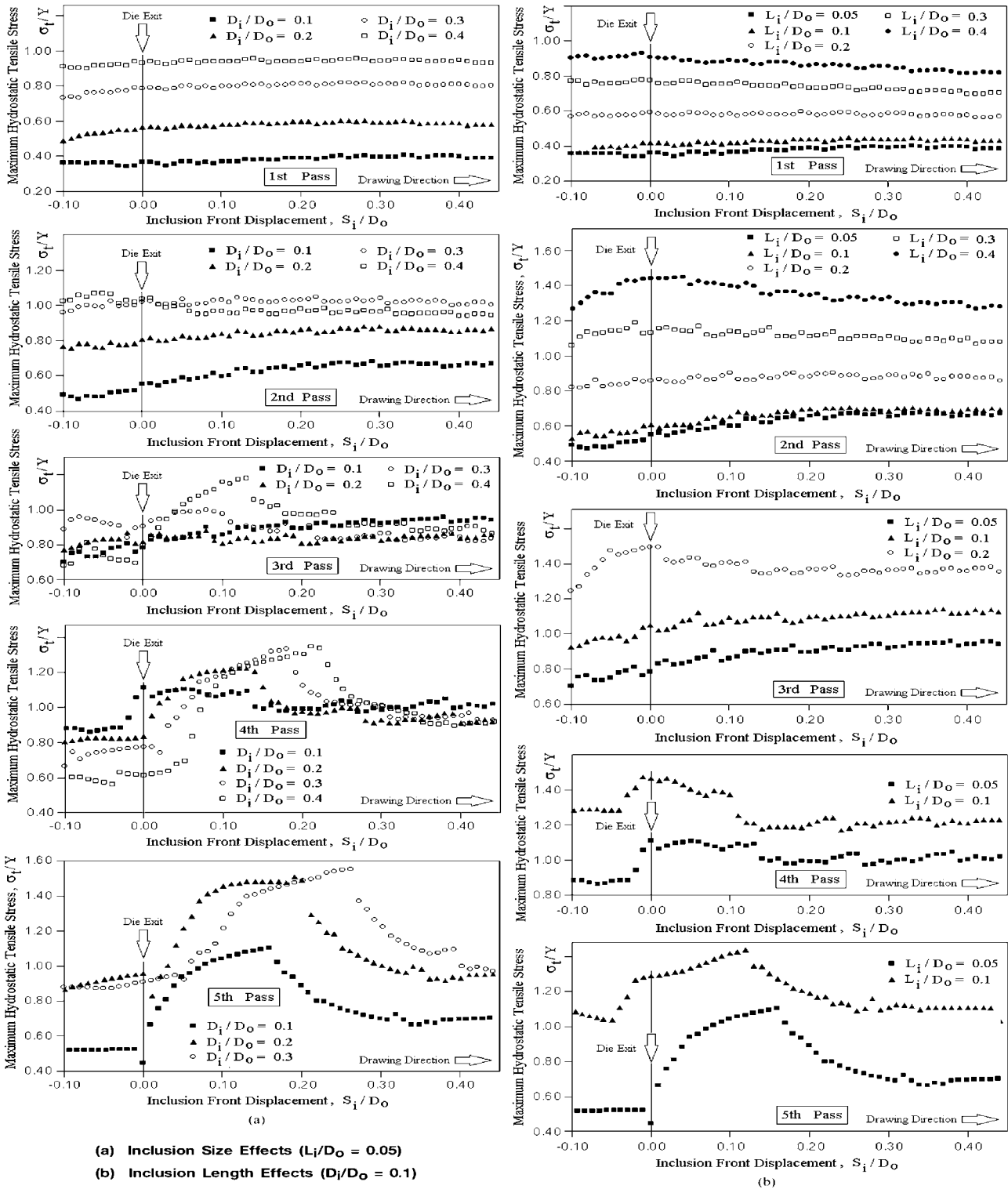


**Figure 6.** Variation of maximum hydrostatic tensile stress ( $\sigma_t/D_0$ ) with inclusion front displacement ( $S_i/D_0$ ) for copper shaped-wire drawing where  $\alpha = 8^\circ$  and  $R/P = 20\%$ .

and was under very slight influence of  $S_i/D_0$ ,

while the inclusion passes through the die.

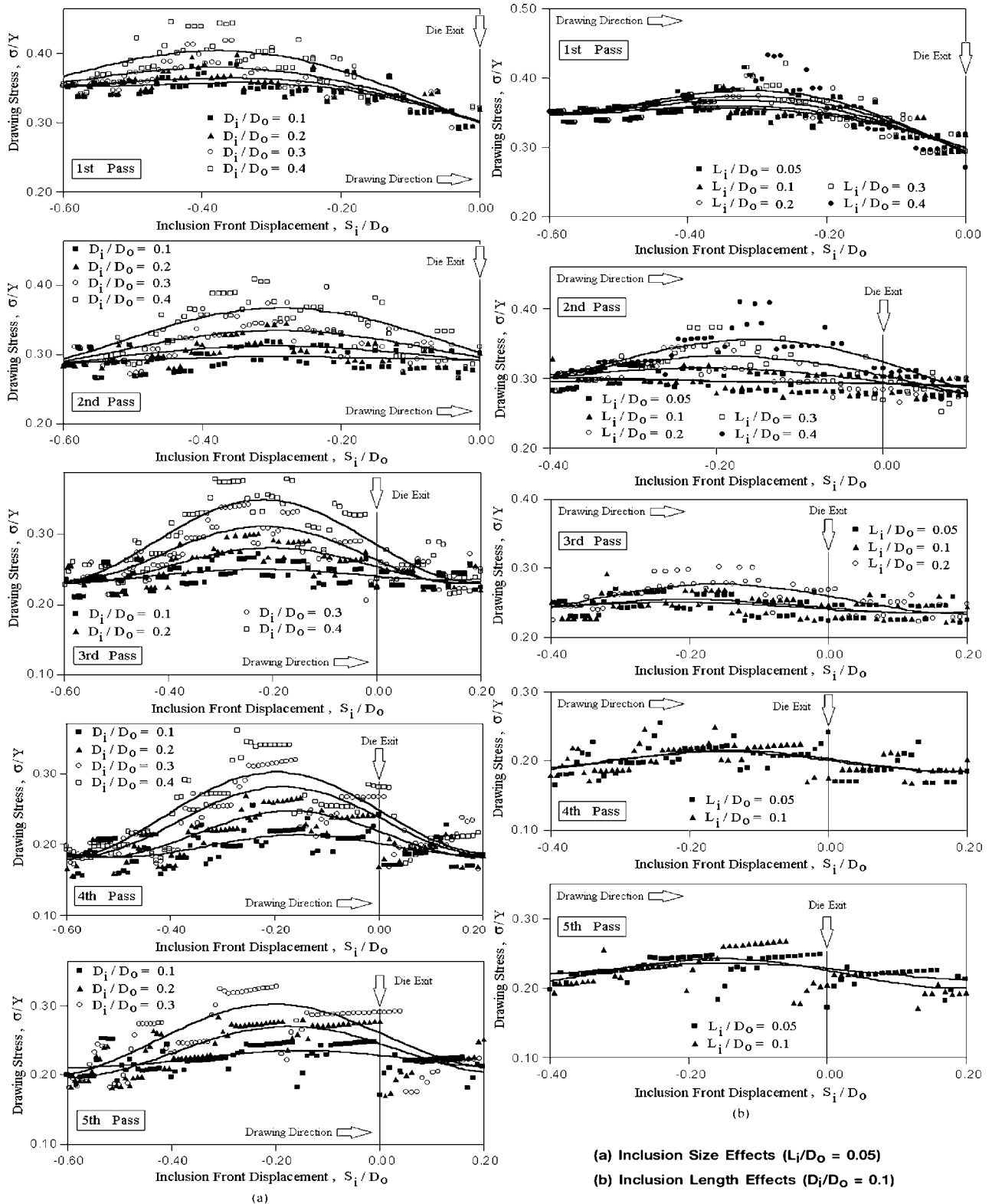


Figure 7. Variation of drawing stress ( $\sigma/D_0$ ) with inclusion front displacement ( $S_i/D_0$ ) for copper shaped-wire drawing where  $\alpha = 8^\circ$  and  $R/P = 20\%$ .

After inclusion exits the die, the  $\sigma_i/Y$  increase until higher than  $\sigma_i/Y$  in case of smaller inclusion and highest at  $S_i/D_o = 0.13$  then decrease as shown in Figure 6 (a).

The  $\sigma_i/Y$  ratio, in case of all smaller inclusions, increases as  $D_i/D_o$  increases. The highest  $\sigma_i/Y$  occurred where inclusion front was out off die and more far away from die exit as  $D_i/D_o$  decrease. In forth pass drawing, the  $\sigma_i/Y$  decrease as  $D_i/D_o$  increase and was slightly influenced by  $S_i/D_o$  while inclusion passes through the die. After inclusion exits the die that behavior were inversion and the  $\sigma_i/Y$  increase as  $S_i/D_o$  increase until highest then decrease. The highest  $\sigma_i/Y$  occurred where inclusion front was out off die and more far away from the die exit as  $D_i/D_o$  and  $S_i/D_o$  increase as shown in Figure 6 (a). In fifth pass drawing, the effect of  $D_i/D_o$  on  $\sigma_i/Y$  still the same behavior as in forth pass drawing but in case of  $D_i/D_o = 0.4$  wire break occurred.

It can be seen that the  $\sigma/Y$  increases as  $D_i/D_o$  increase and the maximum  $\sigma/Y$  was occurred in the drawing zone during inclusion passes through the die as shown in Figure 7(a). Comparing inclusion size and length effects indicates that the  $D_i/D_o$  has more influence on  $\sigma/Y$  than that on  $L_i/D_o$ .

**Inclusion Length Effects** In first pass drawing, the inclusion was also negligibly deformed because of its length and hardness, resulting in very large copper deformation. The inclusion deformation slightly occurred when copper shaped-wire was repeatedly drawn and it was deformed to be “barrel” shape. In case of large and long inclusion, the bending of inclusion was not occurred. Variation of  $\sigma_i/Y$  with  $S_i/D_o$  of copper shaped-wire containing a various length inclusion: 0.05, 0.1, 0.2, 0.3 and 0.4 where  $D_i/D_o = 0.1$  during the whole five times of drawing pass were obtained as shown in Figure 6(b). Figure 7(b) shown the variation of  $\sigma/Y$  with  $S_i/D_o$  of those wires. As the inclusion passes through the die, necking due to an inclusion wire drawing occurred at some parts of the wire. Necking also occurred on the copper shaped-wire surface in front of inclusion near inclusion boundary and its magnitude increase as  $L_i/D_o$  increase. While drawing the wire containing an inclusion, it was

found that the  $\sigma_i/Y$  in front of the inclusion increase as  $L_i/D_o$  increase.

The  $\sigma_i/Y$  increases as  $L_i/D_o$  increase as shown in Figure 6 (b). The inclusion front displacement ( $S_i/D_o$ ) slightly influenced on  $\sigma_i/Y$  in first pass drawing and influenced on  $\sigma_i/Y$  in second and third pass drawing. The highest  $\sigma_i/Y$  occurred where inclusion front was out off die and more far away from die exit as  $L_i/D_o$  decrease. In third pass drawing, wire break occurred for  $L_i/D_o = 0.3$  and 0.4. In forth and fifth pass drawing, the  $\sigma_i/Y$  increase as  $L_i/D_o$  increase and was very slightly influenced by  $S_i/D_o$  during inclusion passes through the die. After inclusion exits the die, the  $\sigma_i/Y$  increase as  $S_i/D_o$  increase until highest then decreases. The highest  $\sigma_i/Y$  occurred where inclusion front was out off die and more far away from the die exit as  $L_i/D_o$  decrease and  $S_i/D_o$  increase and wire break occurred for  $L_i/D_o = 0.2, 0.3$  and 0.4 as shown in Figure 6 (b). If compare between inclusion size and length effects, the  $L_i/D_o$  has more influenced on  $\sigma_i/Y$  than  $D_i/D_o$ .

The  $\sigma/Y$  increases as  $L_i/D_o$  increase and the maximum  $\sigma/Y$  was also occurred in the drawing zone during inclusion passes through the die as shown in Figure 7 (b).

**Drawing Pass Effects** The wire deformation, inclusion deformation and maximum  $\sigma_i/Y$  increase as repeatedly drawn times increase as shown in Figure 5 and 6. The  $\sigma/Y$  decrease as repeatedly drawn times increase from first to forth pass drawing and slightly increase in fifth pass drawing as shown in Figure 7.

**Drawing Stress Behavior** When the high drawing stress occurred while wire drawing, wire breakage easily occurred. The drawing stress ( $\sigma/Y$ ), the ratio of drawing stress of wire containing an inclusion to yield stress, as an inclusion passes through the die was shown in Figure 7. We found that the  $L_i/D_o$  and  $D_i/D_o$  slightly influenced on  $\sigma/Y$  where  $L_i/D_o$  less than 0.2.

For  $L_i/D_o$  was between 0.2 and 1.0, the  $L_i/D_o$  strongly influenced on  $\sigma/Y$  and  $\sigma/Y$  rapidly increase as  $L_i/D_o$  increase. The  $L_i/D_o$  did not influence on  $\sigma/Y$  where  $L_i/D_o$  greater than 1.0. It means that the  $\sigma/Y$  was not affected by  $L_i/D_o$  if  $L_i/D_o$  was greater than 1.0.

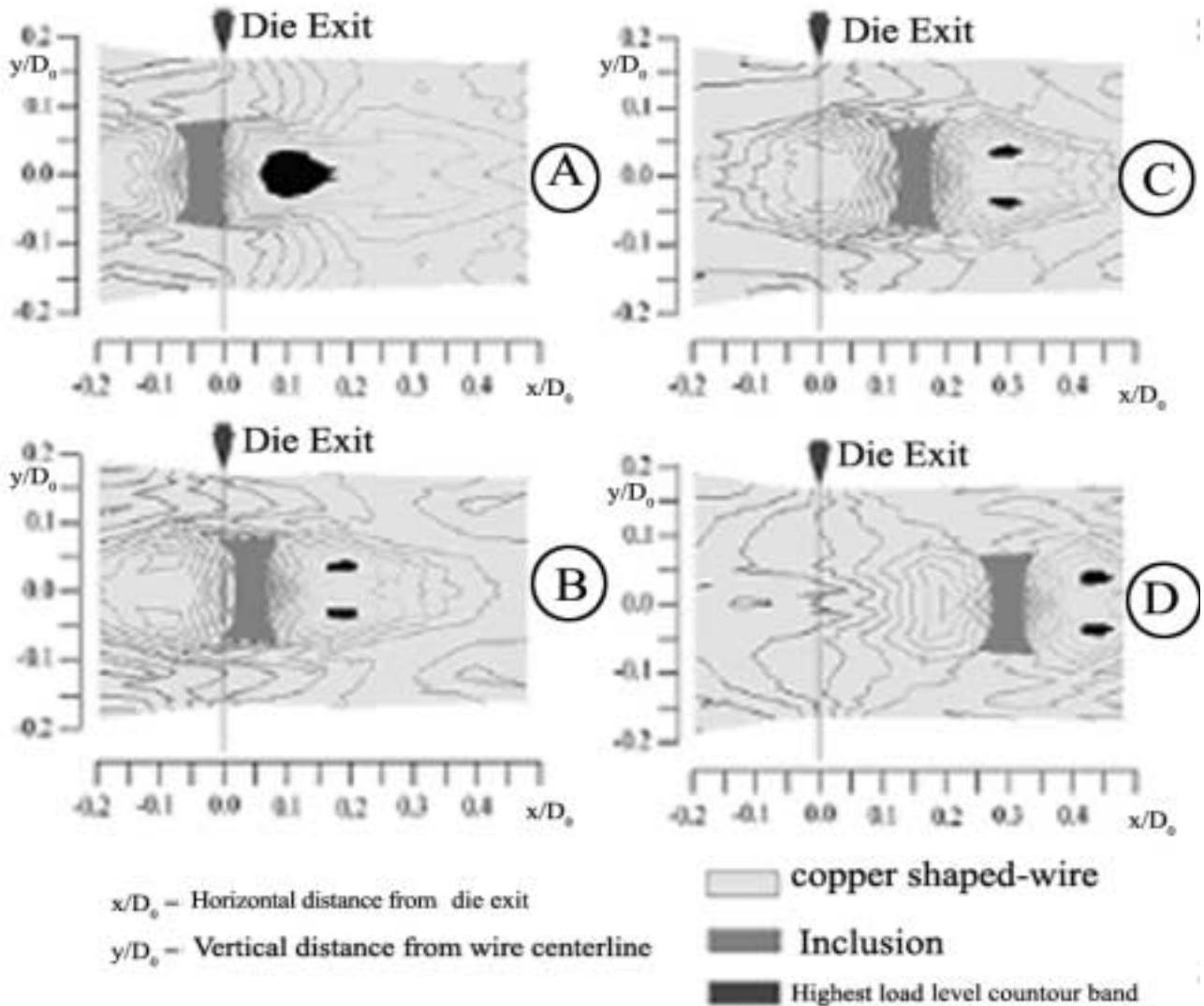


**Figure 8.** Magnitude and location of maximum hydrostatic tensile stress ( $\sigma_t/D_0$ ) in copper shaped-wire containing an inclusion during multi-pass drawing where  $L_i/D_0 = 0.05$ ,  $\square = 8\square$  and  $R/P = 20\%$ .

**Inclusion Length Effects** In first pass drawing, the inclusion was also negligibly deformed because of its length and hardness, resulting in very large copper deformation. The inclusion deformation slightly occurred when copper shaped-wire was repeatedly drawn and it was deformed to be “barrel” shape. In case of large and long inclusion, the bending of inclusion was not occurred. Variation of  $\sigma_t/Y$  with  $S_i/D_0$  of copper shaped-wire containing a various length

inclusion: 0.05, 0.1, 0.2, 0.3 and 0.4 where  $D_i/D_0 = 0.1$  during the whole five times of drawing pass were obtained as shown in Figure 6(b). Figure 7(b) shown the variation of  $\sigma_t/Y$  with  $S_i/D_0$  of those wires. As the inclusion passes through the die, necking due to an inclusion wire drawing occurred at some parts of the wire. Necking also occurred on the copper shaped-wire surface in front of inclusion near inclusion boundary and its magnitude increase as  $L_i/D_0$  increase. While

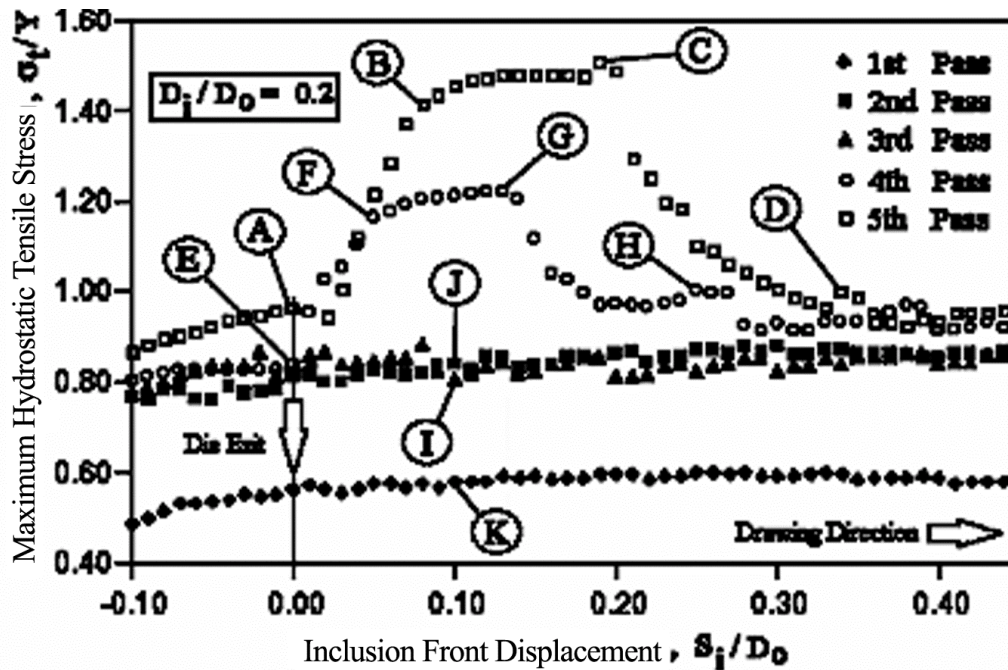


**Figure 8.** Magnitude and location of maximum hydrostatic tensile stress ( $S_i/D_0$ ) in copper shaped-wire containing an inclusion during multi-pass drawing where  $L_i/D_0 = 0.05$ ,  $\square = 8\mu$  and  $R/P = 20\%$ .

drawing the wire containing an inclusion, it was found that the  $\sigma_t/Y$  in front of the inclusion increase as  $L_i/D_0$  increase.

The  $\sigma_t/Y$  increases as  $L_i/D_0$  increase as shown in Figure 6 (b). The inclusion front displacement ( $S_i/D_0$ ) slightly influenced on  $\sigma_t/Y$  in first pass drawing and influenced on  $\sigma_t/Y$  in second and third pass drawing. The highest  $\sigma_t/Y$  occurred where inclusion front was out off die and more far away from die exit as  $L_i/D_0$  decrease. In third pass drawing, wire break occurred for  $L_i/D_0 = 0.3$  and  $0.4$ . In fourth and fifth pass drawing, the  $\sigma_t/Y$  increase as  $L_i/D_0$  increase and was very slightly influenced by  $S_i/D_0$  during inclusion passes through the die. After inclusion exits the die, the  $\sigma_t/Y$  increase as  $S_i/D_0$  increase until highest then decreases. The highest  $\sigma_t/Y$  occurred where inclusion front was out off die and more far away from the die exit as  $L_i/D_0$  decrease and  $S_i/D_0$  increase and wire break occurred for  $L_i/D_0 = 0.2$ ,  $0.3$  and  $0.4$  as shown in Figure 6 (b). If compare between inclusion size and length effects, the  $L_i/D_0$  has more influenced on  $\sigma_t/Y$  than  $D_i/D_0$ .

The  $\sigma_t/Y$  increases as  $L_i/D_0$  increase and the maximum  $\sigma_t/Y$  was also occurred in the drawing

zone during inclusion passes through the die as shown in Figure 7 (b).

**Drawing Pass Effects** The wire deformation, inclusion deformation and maximum  $\sigma_t/Y$  increase as repeatedly drawn times increase as shown in Figure 5 and 6. The  $\sigma_t/Y$  decrease as repeatedly drawn times increase from first to fourth pass drawing and slightly increase in fifth pass drawing as shown in Figure 7.

**Drawing Stress Behavior** When the high drawing stress occurred while wire drawing, wire breakage easily occurred. The drawing stress ( $\sigma_t/Y$ ), the ratio of drawing stress of wire containing an inclusion to yield stress, as an inclusion passes through the die was shown in Figure 7. We found that the  $L_i/D_0$  and  $D_i/D_0$  slightly influenced on  $\sigma_t/Y$  where  $L_i/D_0$  less than  $0.2$ .

For  $L_i/D_0$  was between  $0.2$  and  $1.0$ , the  $L_i/D_0$  strongly influenced on  $\sigma_t/Y$  and  $\sigma_t/Y$  rapidly increase as  $L_i/D_0$  increase. The  $L_i/D_0$  did not influence on  $\sigma_t/Y$  where  $L_i/D_0$  greater than  $1.0$ . It means that the  $\sigma_t/Y$  was not affected by  $L_i/D_0$  if  $L_i/D_0$  was greater than  $1.0$ .

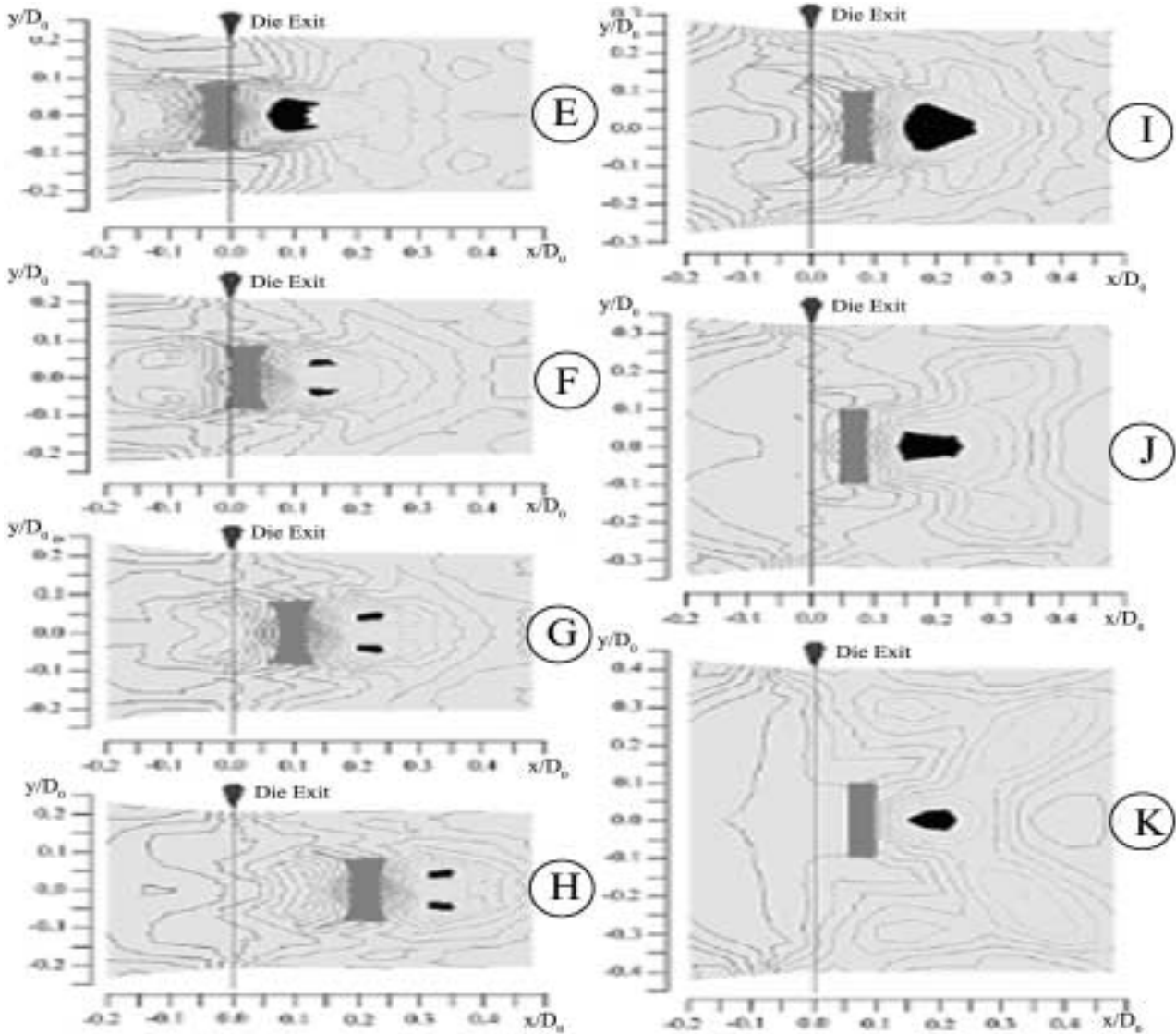


**Figure 8.** Magnitude and location of maximum hydrostatic tensile stress ( $\sigma_t/Y$ ) in copper shaped-wire containing an inclusion during multi-pass drawing where  $L_i/D_0 = 0.05$ ,  $\square = 8\mu$  and  $R/P = 20\%$ .

### Maximum Hydrostatic Tensile Stress Behavior

The magnitude and location of  $\sigma_t/Y$  as an inclusion passes through the die where  $L_i/D_0 = 0.05$  were shown in Figure 8. The black regions were the highest contour band of hydrostatic stress occurred in copper shaped-wire. The dark gray regions were inclusion. The gray regions were copper shaped-wires. The numbers of drawing pass strongly influence on  $\sigma_t/Y$  in forth and fifth pass drawing. The  $S_i/D_0$  strongly influenced on  $\sigma_t/Y$  as a pulse

relationship of  $\sigma_t/Y$  and  $S_i/D_0$  where inclusion front exit the die and  $S_i/D_0$  was between 0.0 to 0.4. In first to third pass drawing, the  $S_i/D_0$  very slightly influenced on  $\sigma_t/Y$ . The  $\sigma_t/Y$  occurred on wire centerline, the centroid of black region, as shown in Figure 8. When the high  $\sigma_t/Y$  occurred while wire drawing, the internal central crack or chevron-crack easily occurred in this location.

The  $L_i/D_0$  strongly influenced on  $\sigma_t/Y$  where  $L_i/D_0$  less than 0.2. The  $\sigma_t/Y$  rapidly increases as

$L_i/D_0$  and  $D_i/D_0$  increase. For  $L_i/D_0$  was between 0.2 and 1.0, the  $L_i/D_0$  influenced on  $\sigma_t/Y$  and influenced transition of  $D_i/D_0$  from directly to inversely influence on  $\sigma_t/Y$  was occurred. The  $\sigma_t/Y$  was not effected by  $L_i/D_0$  when  $L_i/D_0$  greater than 1.0. But  $D_i/D_0$  inversely strong influences on  $\sigma_t/Y$ .

In forth and fifth pass drawing, the two symmetrically located  $\sigma_t/Y$  occurred on both side of wire centerline, two symmetrical black regions, as shown in Figure 8 (B), (C), (D), (F), (G) and (H). In this case, the highest  $\sigma_t/Y$  increase and its location were out off die and more far away from die exit as repeatedly drawn times increase as shown in Figure 8 (C) and (G). The  $\sigma_t/Y$  that occurred on these two symmetrical black regions was very high. The internal double symmetrical cracks easily occurred on the centroid of those two symmetrical black regions.

## 5. CONCLUSIONS

Numbers of drawing pass, inclusion length, inclusion size, inclusion properties and wire properties influence on the inclusion deformation, wire deformation and maximum hydrostatic tensile stress. Necking due to an inclusion wire drawing occurred at some parts of the wire. The inclusion was negligibly deformed in first pass drawing. The inclusion was deformed to be: “crown” shape and bent for large and short inclusion; inverted “crown” shape and unbent for small and short inclusion; and “barrel” shape and unbent for large and long inclusion.

The  $D_i/D_0$  and  $L_i/D_0$  directly influenced on  $\sigma_t/Y$  in first and second pass drawing. The  $S_i/D_0$  slightly influenced on  $\sigma_t/Y$  in first pass drawing and directly influenced on  $\sigma_t/Y$  in second and third pass drawing. In forth and fifth pass drawing, the  $S_i/D_0$  strongly influenced on  $\sigma_t/Y$  as a pulse relationship of  $\sigma_t/Y$  and  $S_i/D_0$  where inclusion front exit the die and  $S_i/D_0$  was between 0.0 and 0.4. Pulse relationship between  $\sigma_t/Y$  and  $S_i/D_0$  where  $D_i/D_0 = 0.4$  occurred, resulting two symmetrically located  $\sigma_t/Y$  occurred on both side of wire centerline. The highest  $\sigma_t/Y$  where  $D_i/D_0 = 0.4$  occurred at  $S_i/D_0 = 0.13$  in third pass drawing. The  $\sigma_t/Y$  that occurred on these two symmetrical

locations was very high. It also occurred for all  $D_i/D_0$  in forth and fifth passes drawing.

The  $D_i/D_0$  directly influence on the  $\sigma_t/Y$ . The maximum  $\sigma_t/Y$  was occurred in the drawing zone during inclusion passes through the die. The  $L_i/D_0$  and  $D_i/D_0$  slightly influenced on  $\sigma_t/Y$  where  $L_i/D_0 < 0.2$ . For  $L_i/D_0$  was between 0.2 and 1.0, the  $L_i/D_0$  strongly influenced on  $\sigma_t/Y$ . The  $L_i/D_0$  did not effect on the  $\sigma_t/Y$  if  $L_i/D_0 > 1.0$ . Wire break occurred where  $D_i/D_0 = 0.4$  in fifth pass drawing and  $L_i/D_0 = 0.3$  and  $0.4$  in forth and fifth pass drawing.

The repeatedly drawn times strongly influenced on  $\sigma_t/Y$  in forth and fifth pass drawing. They inversely and directly influenced on the  $\sigma_t/Y$  in first-to-forth and fifth pass drawing, respectively.

## 6. ACKNOWLEDGMENTS

The authors wish to express appreciation to Director of National Metal and Materials Technology Center (MTEC), National Science and Technology Development Agency, Thailand, for his support and assistance in many details of the finite element program "MSC.MARC" for this problem simulation. The authors would like to thank Mr. R. Ido, Department of Precision Mechanics, School of Engineering, Tokai University 1117 Kitakaname, Hiratsuka, Kanagawa, Japan 259-1292 and Mr. Nissapakul P., Department of Mechanical Engineering, Faculty of Engineering, King Mongkut's Institute of Technology, Ladkrabang, Bangkok 10520, Thailand, for valuable discussions and comments.

## 7. REFERENCES

1. Yoshida, K., “FEM Analysis of Wire Breaks in Drawing of Superfine Wire with An Inclusion”, *Wire Journal International*, (March 2000), 102-107.
2. Mielnik, E. M., “Metalworking Science and Engineering”, McGraw-Hill, New York, (1991), 397-462.
3. Avitzur, B., “Study of Flow Through Conical Converging Dies, Metal Forming”, A. L. Hoffmanner (ed.), Plenum Press, New York, (1971), 1-46.

4. Avitzur, B., "Metal Forming: Processes and Analysis", McGraw-Hill, New York, (1968), 153-258. Revised Edition Reprinted by Robert Krieger, (1979), Publishing Co., Inc., Huntington, N.Y.
5. Avitzur, B., "Analysis of Central Bursting Defects in Extrusion and Wire Drawing", *Trans. ASME*, Ser. B, (1968), 79-91.
6. Coffin, L. F. and Roger, H. C., *Trans. ASME*, Vol. 60, (1967), 672-686.
7. Yoshida, K., "Study on Copper Defects in Wire Drawing", Doctor Dissertation at Tokai University, Japan, (1982).
8. Chen, C. C., Oh, S. I. and Kobayashi, S., "Ductile Fracture in Axisymmetric Extrusion and Drawing", *Trans. ASME*, Ser. B, Vol. 101, (1979), 23-44.
9. Tanaka, H. and Yoshida, K., "Relation Between Oxygen Contents and the Cupping of Tough Pitch Copper Wire", *Journal of the Japan Institute of Metals*, Vol. 43, (1979), 618-625.
10. Yoshida, K. and Tanaka, H., "Cup-Shaped Defect in Copper Wires Drawn from Rods of Continuous Casting and Rolling", *Advanced Technology of Plasticity*, Germany, (1987), 857-862.
11. Raskin, C., *Proceedings of the WAI International Technical Conference*, Italy, (1997).
12. Nikkei-Mechanical, "The Motor Efficiency Competition", Nikkei, Inc., Tokyo, (2000), 40-44.
13. Norasethasopon, S. and Tangsri, T., "Experimental Study of the Effect of a Half-Die Angle on Drawing Stress During Wire Drawing", *Ladkrabang Engineering Journal*, Vol. 18, (2001), 134-139.